UDC 621.313.3

CRITICAL LOADS OF INDUCTION GENERATORS WITH SERIES SELF-EXCITATION

O. Kiselychnyk, M. Pushkar
National Technical University of Ukraine "Kiev Polytechnic Institute"
prosp. Peremohy, 37, Kiev, 03056, Ukraine. E-mail: koi.fea.kpi@gmail.com, pushkar.mykola@gmail.com
M. Bodson
University of Utah
50 South Central Camp. Dr. Rm. 3280, Salt Lake City, UT 84112-9206, USA. E-mail: bodson@eng.utah.edu

The paper develops analytic conditions for series-connected self-excitated induction generators, based on the results obtained for shunt self-excitation. Formulas for critical loads of the generator with series self-excitation are obtained as a function of capacitance and angular frequency. Features of the series self-excitation boundaries compared to the boundaries for the shunt case are shown in plots for computed and experimental data. Computed three-dimensional plots of critical loads are also presented for both cases. It is found that the critical load as a function of the capacitance and velocity does not exhibit an extremum point under series self-excitation, as opposed to the shunt case.

Key words: induction generator, series self-excitation, critical load, self-excitation boundary.

КРИТИЧНІ НАВАНТАЖЕННЯ АСИНХРОННИХ ГЕНЕРАТОРІВ З ПОСЛІДОВНИМ САМОЗБУДЖЕННЯМ

О. І. Кіселичник, М. В. Пушкар
Національний технічний університет України "Київський політехнічний інститут"
просп. Перемоги, 37, Київ, 03056, Україна. E-mail: koi.fea.kpi@gmail.com, pushkar.mykola@gmail.com
М. Бодсон
Університет Юти
50 South Central Camp. Dr. Rm. 3280, Солт Лейк Сіті, UT 84112-9206, США. E-mail: bodson@eng.utah.edu

Представлено аналітичні умови для послідовного самозбудження асинхронних генераторів, отримані на основі результатів для паралельного самозбудження. Виведено формули для розрахунку критичного навантаження генератора з послідовним самозбудженням у функціях ємності та кутової частоти. Показано особливості границь послідовного самозбудження в порівнянні з паралельним. Представлено розрахункові та експериментальні графіки границь самозбудження, а також розрахункові тривимірні графіки критичного навантаження для обох варіантів самозбудження. Виявлено, що при послідовному самозбудженні, на відміну від паралельного, залежність критичного навантаження від ємності та швидкості не має точки екстремуму.

Ключові слова: асинхронний генератор, послідовне самозбудження, критичне навантаження, границя самозбудження.

PROBLEM STATEMENT. Self-excited induction generators (SEIG) have found applications in renewable energy (wind and hydro). One of the challenges of power generating systems based on SEIG's is their poor voltage and frequency regulation in the presence of load changes. An approach to improve voltage regulation is to provide reactive power for SEIG excitation not only from shunt (parallel) capacitors, but also from series capacitors [1], [2]. If series capacitors are connected between the load and the shunt capacitors, one talks of a short-shunt configuration. When series capacitors are placed between the shunt capacitors and the generator, one talks of a long-shunt configuration. The voltage of series capacitors varies with the load current, resulting in lower deviations of the load voltage from a rated value.

The model of the SEIG with short or long shunt is nonlinear and of dimension eight. [1] and [2] present results concerning only voltage regulation, leaving open the problem of self-excitation conditions and load limits. These issues were addressed in [3]–[8] for the case of shunt excitation, utilizing the fact that the matrix differential equation of SEIG's has a special symmetric structure allowing to reduce the order of the system by a factor of 2. The present paper makes a first step towards analysis of long/short shunt configurations by considering the case of pure series self-excitation. Objectives of the paper are to obtain analytic conditions and critical loads for series self-excitation and to study their features compared to shunt self-excitation.

EXPERIMENTAL PART AND RESULTS OBTAINED. 1. *Self-excitation boundaries of induction generator.* Consider a two-phase induction generator with resistive loads connected in parallel with shunt capacitors to the stator windings. The self-excitation boundary of the generator is described by the quartic equation [3], [5]

$$f_1\omega_e^4 + f_2\omega_e^2 + f_3 = 0, \qquad (1)$$

where

$$f_1 = C^2 L_S (L_S L_R - L_M^2) > 0,\ f_3 = L_R (Y_L R_S + 1)^2 > 0,$$
$$f_2 = Y_L^2 L_S (L_S L_R - L_M^2) + C^2 R_S^2 L_R - C(2L_S L_R - L_M^2)$$

with $L_S = L_{\sigma S} + L_M$, $L_R = L_{\sigma R} + L_M$.

The following notation is used: ω_e is the angular electrical frequency, C is the capacitance, Y_L is the admittance of the resistive load, $L_{\sigma S}$ and $L_{\sigma R}$ denote the stator and rotor leakage inductances, L_S and L_R denote the stator and rotor inductances, and R_S is the stator resistance.

Fig. 1 shows the general shape of the magnetization inductance L_M as a function of the magnitude of the magnetizing current i_M [7]. The curve includes an ascending part rising from L_{M0} to L_{MAX}, a flat part at

L_{MAX} corresponding to a linear magnetic regime, and a descending part corresponding to magnetic saturation.

Figure 1 – The magnetization inductance as a function of magnetizing current

The quartic equation is a quadratic equation in ω_e^2, which has a real positive solution if and only if

$$f_2 < -2\sqrt{f_1 f_3}\,. \qquad (2)$$

If (2) is satisfied, there are two real positive solutions to the quadratic equation, and we denote the two square roots of these solutions $\omega_{e,\min}$ and $\omega_{e,\max}$. These are the solutions of the quartic equation. The velocity ω can be determined from ω_e using [3], [5]

$$\omega = \frac{1}{n_P}\left(\omega_e - \frac{Y_L R_S R_R - \omega_e^2 C R_R L_S + R_R}{\omega_e\left(Y_L\left(L_S L_R - L_M^2\right) + R_S L_R C\right)}\right), \qquad (3)$$

where n_p denotes the number of pole pairs.

From $\omega_{e,\min}$ and $\omega_{e,\max}$, velocities $\omega_{\min}$ and $\omega_{\max}$ can be determined in this manner. The velocities constitute the boundaries where self-excitation is possible. If the procedure is applied with $L_M = L_{MAX}$, the boundaries of self-excitation (which may require triggering to be reached) are obtained. If $L_M = L_{M0}$ is used, the boundaries of spontaneous self-excitation are obtained [3]–[5].

The model of the two-phase SEIG with only series excitation capacitors and resistive loads is a special case of the model for the shunt self-excitation case. One simply removes the load by letting $Y_L=0$ in the analysis and include the load instead with the stator resistance, replacing R_S by $R_S + R_L$. Applying the approach from [3]–[8] then gives analytic conditions for series self-excitation as follows. Substituting $Y_L = 0$ and $R_S = R_S + R_L$ into (1) and (3) gives the analytic expressions for series self-excitation boundaries

$$f_1\omega_e^4 + f_2\omega_e^2 + f_3 = 0\,; \qquad (4)$$

$$\omega = \frac{1}{n_P}\left(\omega_e - \frac{R_R - \omega_e^2 C R_R L_S}{\omega_e (R_S + R_L) L_R C}\right), \qquad (5)$$

where $f_1 = C^2 L_S\left(L_S L_R - L_M^2\right) > 0$; $f_3 = L_R > 0$;

$f_2 = C^2 (R_S + R_L)^2 L_R - C\left(2L_S L_R - L_M^2\right)$.

Alternatively, equation (4) can be expressed as the quadratic equation

$$g_1 C^2 - g_2 C + g_3 = 0\,, \qquad (6)$$

where $g_1 = L_S(L_S L_R - L_M^2)\omega_e^4 + (R_S + R_L)^2 L_R \omega_e^2 > 0$;

$g_2 = (2L_S L_R - L_M^2)\omega_e^2 > 0$, $g_3 = L_R > 0$.

The quadratic equation has two real positive solutions if and only if

$$g_2^{\,2} - 4g_1 g_3 > 0\,. \qquad (7)$$

The solutions of the quadratic equation for given R_L and ω_e are $C_{\min}$ and $C_{\max}$. Substitution them into equation (5) gives $\omega_{\min}$ and $\omega_{\max}$.

2. *Critical load of induction generator with series self-excitation for different frequencies.* Rewrite equation (4) as follows

$$a_1 R_L^2 + a_2 R_L + a_3 = 0\,, \qquad (8)$$

where $a_1 = C^2 L_R \omega_e^2 > 0$, $a_2 = 2C^2 L_R \omega_e^2 R_S > 0$;

$a_3 = C^2(L_S(L_S L_R - L_M^2)\omega_e^4 + R_S^2 L_R \omega_e^2) -$

$-\,C(2L_S L_R - L_M^2)\omega_e^2 + L_R$.

Equation (8) has a single solution

$$R_L = \left(-a_2 + \sqrt{a_2^2 - 4a_1 a_3}\right)/(2a_1)\,, \qquad (9)$$

that is positive or zero if and only if $a_3 \le 0$.

The last inequality can be expressed as

$$a_3(C) = b_1 C^2 - b_2 C + b_3 \le 0\,, \qquad (10)$$

where

$b_1 = g_1(R_L = 0) = L_S(L_S L_R - L_M^2)\omega_e^4 + R_S^2 L_R \omega_e^2 > 0$;

$b_2 = g_2 = (2L_S L_R - L_M^2)\omega_e^2 > 0$, $b_3 = g_3 = L_R > 0$.

The function $a_3(C)$ is negative or zero for all capacitance values between the two solutions of quadratic equation (10)

$$C_{1,2} = \left(b_2 \pm \sqrt{b_2^2 - 4b_1 b_3}\right)/(2b_1) \qquad (11)$$

if and only if $b_2^2 - 4b_1 b_3 \ge 0$. Note that the values $C = C_{1,2}$ correspond to the case with $R_L = 0$.

Substituting b_1, b_2 and b_3 into the last inequality gives the minimum possible generated angular frequency

$$\omega_e \ge 2L_R R_S / L_M^2\,, \qquad (12)$$

which is the same value as for the case with shunt self-excitation. Substitution of $L_M = L_{MAX}$ gives minimum operating frequency.

Equation (9) can be put in the form

$$R_L = -R_S + \sqrt{f(C, \omega_e)}\,, \qquad (13)$$

where

$$f = \frac{C(2L_S L_R - L_M^2)\omega_e^2 - L_R - C^2 L_S (L_S L_R - L_M^2)\omega_e^4}{C^2 L_R \omega_e^2}.$$

The maximum value of the load R_L in (13) corresponds to a maximum value of $f(C, \omega_e)$. Equating $\partial f(C, \omega_e)/\partial C$ to zero gives the value of capacitance

$$C_{ex} = \frac{2L_R}{(2L_S L_R - L_M^2)\omega_e^2} > 0\,. \qquad (14)$$

Since $\dfrac{\partial^2 f(C = C_{ex}, \omega_e)}{\partial^2 C} = -\dfrac{\omega_e^6 (2L_S L_R - L_M^2)^4}{L_R^4} < 0$, the value C_{ex} corresponds to the maximum of $f(C, \omega_e)$.

Substitution of equation (14) into (13) gives the dependency of the critical loads for different angular frequencies.

$$R_{L\max} = -R_S + \omega_e \frac{L_M^2}{2L_R}\,. \qquad (15)$$

Combining (14) and (15) with equation (5) gives the dependency of the maximum load on the velocity. Note that on the contrary to the shunt self-excitation where the function $Y_{L\max}(\omega_e)$ has a maximum point [6], the function $R_{L\max}(\omega_e)$ is linear.

3. *Critical load of induction generator for different capacitances*. Rewrite inequality (10) in following manner

$$a_3(\omega_e) = d_1\omega_e^4 + d_2\omega_e^2 + d_3 \le 0, \qquad (16)$$

where $d_1 = C^2 L_S(L_S L_R - L_M^2) > 0$; $d_3 = L_R > 0$;
$d_2 = R_S^2 L_R C^2 - C(2L_S L_R - L_M^2)$.

The quartic equation is a quadratic equation in ω_e^2, which has a real positive solution if and only if

$$d_2 < -2\sqrt{d_1 d_3}\,. \qquad (17)$$

If (17) is satisfied, the function $a_3(\omega_e)$ is negative or zero for all angular frequency values between the two solutions of equation (16)

$$\omega_{e1,2} = \sqrt{\left(-d_2 \pm \sqrt{d_2^2 - 4d_1 d_3}\right)/(2d_1)}\,. \qquad (18)$$

Note, that the values $\omega_e = \omega_{e1,2}$ correspond to the no load case $R_L = 0$.

Substituting d_1, d_2 and d_3 into inequality (17) gives the maximum possible capacitance

$$C < \frac{2L_S L_R - L_M^2 - 2\sqrt{L_S L_R(L_S L_R - L_M^2)}}{R_S^2 L_R}, \qquad (19)$$

which is the same value as for the case with shunt self-excitation. Substituting $L_M = L_{MAX}$ gives maximum possible values for operating modes, while $L_M = L_{M0}$ gives values for spontaneous self-excitation.

Equating $\partial f(C,\omega_e)/\partial\omega_e$ to zero gives the value of angular frequency

$$\omega_{eex} = \sqrt[4]{\frac{L_R}{C^2 L_S(L_S L_R - L_M^2)}}\,. \qquad (20)$$

Since $\dfrac{\partial^2 f(C,\omega_e=\omega_{eex})}{\partial^2\omega_e} = -8(L_S L_R - L_M^2)\dfrac{L_S}{L_R} < 0$,

the value ω_{eex} corresponds to the maximum of $f(C,\omega_e)$. Substitution of equation (20) into (13) gives the dependency of the critical loads for different capacitances

$$R_{L\max} = -R_S + \sqrt{\frac{2L_S L_R - L_M^2}{CL_R} - \frac{2}{C}\sqrt{\frac{L_S(L_S L_R - L_M^2)}{L_R}}}\,. \qquad (21)$$

Note that, as opposed to the shunt self-excitation case where the function $Y_{L\max}(C)$ has a maximum point [6], the function $R_{L\max}(C)$ is hyperbolic. In case of the shunt self-excitation, the intersection point of the curves $Y_{L\max}(C_{ex},\omega_e)$ and $Y_{L\max}(C,\omega_{eex})$ in the coordinate frame (C,ω,Y_L) exists [6] and define the general maximum load point.

Equating the right sides of equations (15) and (21) gives following relationship

$$C = \frac{4L_R^2}{L_M^4\omega_e^2}\left(\frac{2L_S L_R - L_M^2}{L_R} - 2\sqrt{\frac{L_S(L_S L_R - L_M^2)}{L_R}}\right). \qquad (22)$$

Substituting either $C = C_{ex}$ from (14) or $\omega_e = \omega_{eex}$ from (20) makes (22) incorrect eliminating ω_e and C from the equation. Therefore, the curves $R_{L\max}(C_{ex},\omega_e)$ and $R_{L\max}(C,\omega_{eex})$ don't intersect.

4. *Computation and experimental results.* A three-phase induction motor (АИРМ63В4У3, with rated values 370W, 380V, 50 Hz, and 1450 rpm) was used for experiments as SEIG. The following parameters of the generator were determined experimentally R_S =27 Ω, R_R =17.9 Ω, $L_{\sigma S} = L_{\sigma R}$ =0.08266 H, n_p =2, L_{MAX} =1.03115 H, L_{M0} =0.6345 H. The SEIG was coupled to another induction motor (4AM80B3Y3, with rated values 2.2KW, 380V, 50 Hz, and 2800 rpm) controlled through the frequency converter ABB ACS140 feeding the stator winding. The higher value of the motor's power and the slip compensation function in the ACS140 provided velocity stabilization at desired levels during experiments. The excitation capacitors were engaged through three-phase relays and a programmable logic relay Lovato Kinco. The loads were Y-connected. Collection of the experimental data was performed using ACS140's monitoring system and a system for tests of electric drives providing voltage and current measurements with visualization compatible with Matlab.

Computed and experimental self-excitation boundaries for SEIG with the series capacitors and different load conditions are shown in Fig. 2.

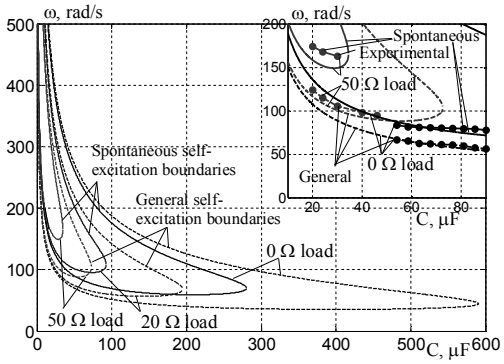

Figure 2 – Series self-excitation boundaries

The spontaneous self-excitation boundaries were computed with $L_M = L_{M0}$ while for the general self-excitation boundaries $L_M = L_{MAX}$. Any operating point inside the corresponding spontaneous boundary provides spontaneous self-excitation. If the point is between the spontaneous and the general boundaries, self-excitation is possible but must be triggered by an external energy source, for example a pre-charged capacitor. The self-excitation sustains until the operating point remains inside the corresponding general self-excitation boundary. During experiments, the general self-excitation boundaries were determined as collapse regions. The SEIG velocity was increased to start spontaneous self-excitation. Then the velocity was reduced

until the voltage collapsed. The result defined the experimental boundary for general self-excitation.

Computed and experimental self-excitation boundaries for SEIG with the shunt capacitors and different load conditions are shown in Fig. 3.

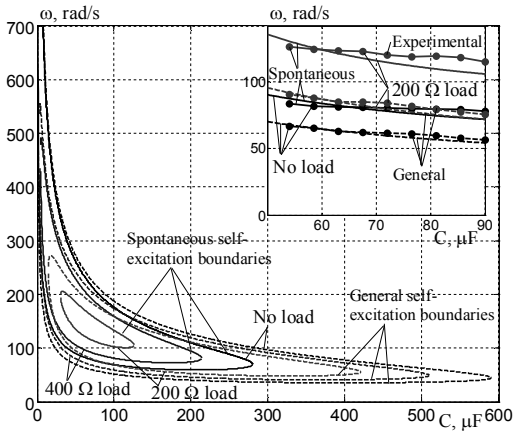

Figure 3 – Shunt self-excitation boundaries

During experiments, the shunt capacitors were Δ-connected, so that their values for plots were tripled to reach the equivalent Y-connection. As expected, the spontaneous and general self-excitation boundaries for the series case with $R_L = 0$ and for the shunt case with $Y_L = 0$ are the same. Increase of R_L for series self-excitation affects the self-excitation boundaries with the same trend as an increase of Y_L for the shunt self-excitation. The difference is that the critical highest velocities do not decrease with increases of R_L, as is the case for Y_L increases under the shunt self-excitation.

Fig. 4 shows a three-dimensional plot of the series self-excitation boundaries based on equation (9) with $L_M = L_{MAX}$. The parabolic function $R_L = f(C)$ was computed for different angular frequencies over the critical value defined by (12) and within the capacitance range defined by (11). The corresponding velocity values were taken from (5). All the operating points of the generator are inside the figure delimited by the surfaces $R_L = f(C, \omega)$ and $R_L = 0$. Curve 1 shows maximum loads for different frequencies according to (15). Curves 2, 3, and 4 are the series self-excitation boundaries for 50 Ω, 20 Ω and 0 Ω load cases respectively computed based on (6). As can be seen from the figure, the curve $R_{L\max} = f(C_{ex}, \omega)$ has no extreme point.

A similar plot for the SEIG in case of the shunt self-excitation is presented in Fig. 5 based on the theory from [6]. Curve 1 shows maximum loads for different frequencies. Curves 2, 3, and 4 are the shunt self-excitation boundaries for 200 Ω, 400 Ω and no load cases respectively. The curve $Y_{L\max}(C_{ex}, \omega)$ has a maximum point 5, and this point is unique [6]

$$C_5 = \frac{L_S(\sqrt{\sigma}-1)^2}{4R_S^2};\ \omega_{e5} = \frac{R_S(1+\sqrt{\sigma})}{L_S\sqrt{\sigma}(1-\sqrt{\sigma})};$$

$$Y_{L5} = \frac{(\sqrt{\sigma}-1)^2}{4R_S\sqrt{\sigma}}, \qquad (23)$$

where $\sigma = \left(L_S L_R - L_M^2\right)/(L_S L_R) > 0$ and ω_5 is computed from (3) with $\omega_e = \omega_{e5}$, $C = C_5$, and $Y_L = Y_{L5}$.

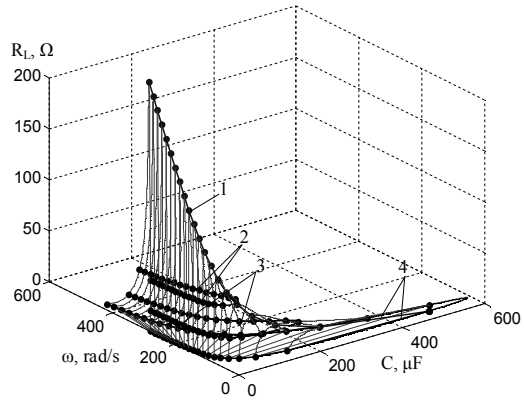

Figure 4 – $R_L = f(C, \omega)$ computed through the range of angular frequencies for series self-excitation

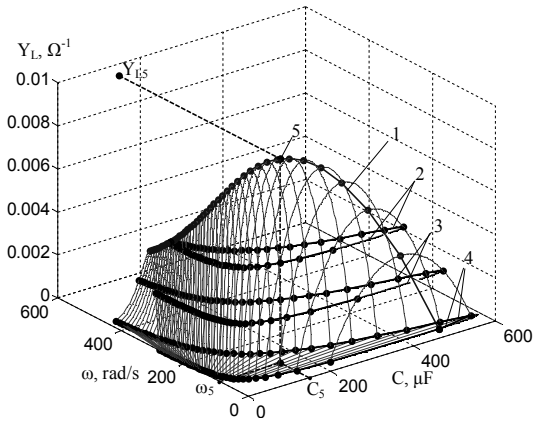

Figure 5 – $Y_L = f(C, \omega)$ computed through the range of angular frequencies for shunt self-excitation

Fig. 6 also shows a three-dimensional plot of the series self-excitation boundaries based on equation (9) with $L_M = L_{MAX}$. This time, the parabolic functions $R_L = f(\omega)$ were computed for capacitances lower than the critical value defined by (19) within the frequency range defined by (18). Curve 1 shows the maximum loads for different capacitances computed according (21). Curves 2, 3, and 4 are the series self-excitation boundaries for the 50 Ω, 20 Ω, and 0 Ω load cases respectively, computed based on (4). The curve $R_{L\max} = f(C, \omega_{ex})$ has no extreme point, where ω_{ex} is computed from (5) with $\omega_e = \omega_{eex}$ and $R_L = R_{L\max}$. Three-dimensional rotations of Figs. 4 and 6 have shown that there were no intersections of the curves $R_{L\max} = f(C, \omega_{ex})$ and $R_{L\max} = f(C_{ex}, \omega)$.

A similar plot for the SEIG with the shunt self-excitation is depicted in Fig. 7 according to [6]. Curve 1 shows maximum loads for different capacitances. Curves 2, 3, and 4 are the shunt self-excitation boundaries for 200 Ω, 400 Ω and no load cases respectively. The curve $Y_{L\max}(C, \omega_{ex})$ intersects the curve $Y_{L\max}(C_{ex}, \omega)$ at maximum point 5 defined by (23).

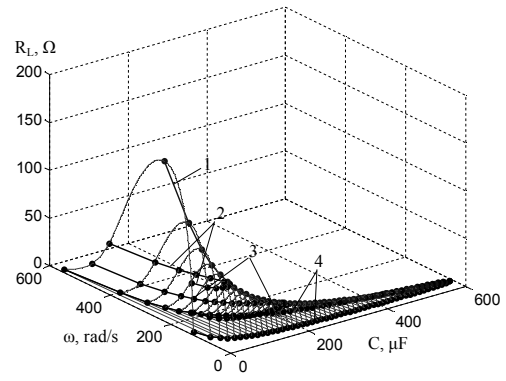

Figure 6 – $R_L = f(C, \omega)$ computed through the range of capacitances for series self-excitation

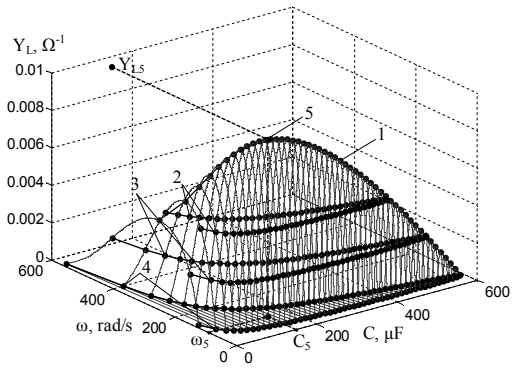

Figure 7 – $Y_L = f(C, \omega)$ computed through the range of capacitances for shunt self-excitation

CONCLUSIONS. The series self-excitation boundaries monotonously shrink inside the boundary for zero resistance when the load resistance increases, resembling the evolution of shunt self-excitation boundaries when the load admittance increases from zero. The minimum possible generating frequency and maximum possible capacitance are the same in both cases, because they correspond to the same configuration. For any specific capacitance or angular frequency inside the corresponding self-excitation boundary, there is an operating point providing maximum loading ability of SEIG. The dependence of the critical load on the capacitance and velocity under series self-excitation, as opposed to shunt excitation, was found to have no extreme point.

REFERENCES

1. Wang L., Su J-Y. Effects of long-shunt and short-shunt connections on voltage variations of a self-excited induction generator // *IEEE Transactions on Energy Conversion.* – 1997. – Iss. 12. – № 4. – PP. 368–374.

2. Singh B., Shridhar L., Jha C.S. Improvements in the performance of self-excited induction generator through series compensation // *IEE Proceedings-Generation, Transmission and Distribution.* – 1999. – Iss. 146. – № 6. – PP. 602–608.

3. Bodson M., Kiselychnyk O. Analysis of triggered self-excitation in induction generators and experimental validation // *IEEE Transactions on Energy Conversion.* – 2012. – Iss. 27 (2). – PP. 238–249.

4. Bodson M., Kiselychnyk O. Nonlinear dynamic model and stability analysis of self-excited induction generators // *Proc. of the American Control Conference, San Francisco, CA, USA.* – 2011. – PP. 4574–4579.

5. Bodson M., Kiselychnyk O. On the capacitor voltage needed to trigger self-excitation in induction generators // *Proc. of 19-th Mediterranean Conference on Control and Automation, Corfu, Greece.* – 2011. – PP. 351–357.

6. Kiselychnyk O., Pushkar M., Bodson M. Critical load of self-excited induction generators // *Electrotechnic and Computer Systems.* – 2011. – № 03 (79). – PP. 282–285.

7. Bodson M., Kiselychnyk O. On the triggering of self-excitation in induction generators // *Proc. of the 20th International Symposium on Power Electronics, Electrical Drives, Automation and Motion (Speedam 2010), Pisa, Italy.* – 2010. – PP. 866–871.

8. Bodson M., Kiselychnyk O. Analytic conditions for spontaneous self-excitation in induction generators // *Proc. of the American Control Conference, Baltimore, MD, USA.* – 2010. – PP. 2527–2532.

КРИТИЧЕСКИЕ НАГРУЗКИ АСИНХРОННЫХ ГЕНЕРАТОРОВ С ПОСЛЕДОВАТЕЛЬНЫМ САМОВОЗБУЖДЕНИЕМ

О. И. Киселичник, Н. В. Пушкарь
Национальный технический университет Украины "Киевский политехнический институт"
просп. Победы, 37, Киев, 03056, Украина. E-mail: koi.fea.kpi@gmail.com, pushkar.mykola@gmail.com
М. Бодсон
Университет Юты
50 South Central Camp. Dr. Rm. 3280, Солт Лейк Сити, UT 84112-9206, США. E-mail: bodson@eng.utah.edu

Представлены аналитические условия для последовательного самовозбуждения асинхронных генераторов, полученные на основе результатов для параллельного самовозбуждения. Выведены формулы для расчетов критической нагрузки генератора с последовательным самовозбуждением в функциях емкости и угловой частоты. Показаны особенности границ последовательного самовозбуждения по сравнению с параллельным. Представлены расчетные и экспериментальные графики границ самовозбуждения, а также расчетные трехмерные графики критической нагрузки для обоих вариантов самовозбуждения. Определено, что при последовательном самовозбуждении, в отличие от параллельного, зависимость критической нагрузки от емкости и скорости не имеет точки экстремума.

Ключевые слова: асинхронный генератор, последовательное самовозбуждение, критические нагрузки, граница самовозбуждения.

Стаття надійшла 16.07.2012.
Рекомендовано до друку
к.т.н., доц. Гладирем А.І.